**Arthritis & Rheumatology**
Vol. 0, No. 0, Month 2023, pp 1–16
DOI 10.1002/art.42462


American College of Rheumatology
Empowering Rheumatology Professionals

# Povetacicept, an Enhanced Dual APRIL/BAFF Antagonist That Modulates B Lymphocytes and Pathogenic Autoantibodies for the Treatment of Lupus and Other B Cell–Related Autoimmune Diseases

Lawrence S. Evans, Katherine E. Lewis, Daniel DeMonte, Janhavi G. Bhandari, Logan B. Garrett, Joseph L. Kuijper, Daniel Ardourel, Martin F. Wolfson, Susan Debrot, Sherri Mudri, Kayla Kleist, Luana L. Griffin, LuAnne Hebb, Russell J. Sanderson, NingXin Wang, Michelle Seaberg, Allison G. Chunyk, Jing Yang, Youji Hong, Zahra Maria, David J. Messenheimer, Pamela M. Holland, Stanford L. Peng, Mark W. Rixon, and Stacey R. Dillon

**Objective.** Dysregulated APRIL/BAFF signaling is implicated in the pathogenesis of multiple autoimmune diseases, including systemic lupus erythematosus and lupus nephritis. We undertook this study to develop and evaluate a high-affinity APRIL/BAFF antagonist to overcome the clinical limitations of existing B cell inhibitors.

**Methods.** A variant of TACI-Fc generated by directed evolution showed enhanced binding for both APRIL and BAFF and was designated povetacicept (ALPN-303). Povetacicept was compared to wild-type (WT) TACI-Fc and related molecules in vitro and in vivo.

**Results.** Povetacicept inhibited APRIL and BAFF more effectively than all evaluated forms of WT TACI-Fc and selective APRIL and BAFF inhibitors in cell-based reporter assays and primary human B cell assays, mediating potent suppression of B cell proliferation, differentiation, and immunoglobulin (Ig) secretion. In mouse immunization models, povetacicept significantly reduced serum immunoglobulin titers and antibody-secreting cells more effectively than anti-CD20 monoclonal antibodies, WT TACI-Fc, or APRIL and BAFF inhibitors. In the NZB × NZW mouse lupus nephritis model, povetacicept significantly enhanced survival and suppressed proteinuria, anti–double-stranded DNA antibody titers, blood urea nitrogen, glomerulonephritis, and renal immunoglobulin deposition. In the bm12 mouse lupus model, povetacicept significantly reduced splenic plasmablasts, follicular helper T cells, and germinal center B cells. In non-human primates, povetacicept was well tolerated, exhibited high serum exposure, and significantly decreased serum IgM, IgA, and IgG levels after a single dose.

**Conclusion.** Enhanced APRIL and BAFF inhibition by povetacicept led to greater inhibition of B cell populations critical for autoantibody production compared to WT TACI-Fc and CD20-, APRIL-, or BAFF-selective inhibitors. Potent, dual inhibition by povetacicept has the potential to significantly improve clinical outcomes in autoantibody-related autoimmune diseases.

## INTRODUCTION

B cells have long been implicated in autoimmune diseases such as systemic lupus erythematosus (SLE), owing to their ability to present antigens to autoreactive T cells, secrete inflammatory cytokines (1), and differentiate into antibody-secreting cells (ASCs), i.e., plasmablasts and plasma cells, that are responsible for the production of pathogenic autoantibodies (2). Therefore, depletion or inhibition of B cells and ASCs represents a compelling approach for treating many rheumatic and other autoimmune disorders.

Key modulators of B cell development, differentiation, and survival include the tumor necrosis factor (TNF) family cytokines

Supported by Alpine Immune Sciences, Inc.

Mr. Evans and Dr. Lewis contributed equally to this work.

Lawrence S. Evans, BSc, Katherine E. Lewis, PhD, Daniel DeMonte, PhD, Janhavi G. Bhandari, MSc, Logan B. Garrett, BSc, Joseph L. Kuijper, BSc, Daniel Ardourel, BSc, Martin F. Wolfson, BSc, Susan Debrot, BSc, Sherri Mudri, BSc, Kayla Kleist, MSc, Luana L. Griffin, BSc, LuAnne Hebb, AAS, MFA, Russell J. Sanderson, PhD, NingXin Wang, BSc, Michelle Seaberg, BSc, Allison G. Chunyk, MSc, Jing Yang, PhD, Youji Hong, BSc, Zahra Maria, PhD, David J. Messenheimer, PhD, Pamela M. Holland, PhD, Stanford L. Peng, MD, PhD, Mark W. Rixon, PhD, and Stacey R. Dillon, PhD: Alpine Immune Sciences, Inc., Seattle, Washington.

Author disclosures and a graphical abstract are available online at https://onlinelibrary.wiley.com/doi/10.1002/art.42462.

Address correspondence via email to Stacey R. Dillon, PhD, at Stacey.Dillon@alpineimmunesciences.com.

Submitted for publication October 27, 2022; accepted in revised form January 24, 2023.

BAFF (TNF superfamily 13B) and APRIL (TNF superfamily 13), which are expressed primarily by myeloid cells and signal through multiple receptors. BAFF binds with varying affinity to B cell–expressed BAFF receptor (BAFF-R; TNF receptor superfamily 13C), TACI (TNF receptor superfamily 13B), and BCMA (TNF receptor superfamily 17), while APRIL binds TACI and BCMA (3) and heparin sulfate proteoglycan. BAFF can exist in 3 functional forms, membrane bound, soluble trimer, and soluble BAFF 60-mer (4), with the soluble trimer formed via proteolytic cleavage of membrane BAFF (3). APRIL and BAFF can also form functionally active heterotrimers (5,6). All forms of these cytokines have been shown to be elevated in various antibody-related diseases, including SLE.

Despite structural similarities and engagement of common signaling pathways, APRIL and BAFF play nonredundant roles in B cell regulation, due in part to differential receptor expression at partially overlapping stages of B cell development. While BAFF has key roles earlier in B cell development when BAFF-R is expressed, APRIL assumes a key role in the function of differentiated ASCs that express TACI, BCMA, and heparin sulfate proteoglycan (e.g., syndecan 1/CD138).

Among several B cell–targeting strategies, blockade of BAFF or APRIL has shown clinical promise. Belimumab is an anti-BAFF antibody approved for the treatment of SLE (7) and SLE-related lupus nephritis (LN) (8), but clinical remission as measured by Lupus Low Disease Activity State (LLDAS) or complete renal response is achieved in only a minority of patients, (12–14% or 30%, respectively) (9,10). Thus, there remains a need for more effective agents. Other BAFF/APRIL-targeting antibodies include ianalumab, a blocking and cell-depleting anti–BAFF-R antibody (11), and the anti-APRIL antibodies BION-1301 (12) and sibeprenlimab (VIS649) (13). These antibodies have demonstrated promising pharmacodynamic activity in phase I clinical trials (14,15), but are limited by only inhibiting either BAFF or APRIL (3,16–21). BAFF-Trap, a wild-type (WT) TACI and WT BAFF-R hybrid Fc fusion protein (22), also shares limitations by inhibiting only BAFF.

Atacicept (3) and telitacicept (23) are soluble WT TACI extracellular domain Fc fusion proteins that strongly inhibit BAFF and weakly inhibit APRIL signaling. Atacicept and telitacicept have both demonstrated clinical efficacy in SLE (23–25). However, atacicept formally failed to meet its primary end point in pivotal trials (24) and appears to no longer be in active development for SLE (26). In contrast, telitacicept has been conditionally approved in China for the treatment of SLE based on a phase IIb study and recent positive confirmatory phase II results; however, most trial patients appeared to have still experienced flares within the first 6 months of treatment (27). These findings provide clinical validation of the BAFF/APRIL pathway for SLE, but also suggest that further improvement upon the drug designs of atacicept and telitacicept, perhaps by improving APRIL inhibition in particular, may afford a unique opportunity to achieve more effective yet safe therapeutic options.

Herein we describe the engineering of a modified TACI domain to generate povetacicept (ALPN-303), a potent inhibitor of both APRIL and BAFF. We show that modifications in the TACI domain of povetacicept translate to enhanced target binding affinity and inhibitory activity compared to WT TACI-Fc in vitro, and greater immunoglobulin (Ig) suppression over comparators in mouse immunization and SLE disease models. We postulate that improved dual APRIL and BAFF inhibition may provide more effective and durable relief from severe autoimmune diseases in which B cells and antibody responses play a role.

## MATERIALS AND METHODS

**Proteins and cell lines.** Recombinant APRIL and BAFF were purchased from Tonbo Biosciences and BioLegend, respectively. BAFF 60-mer was obtained from AdipoGen. Belimumab was either generated on site at Alpine Immune Sciences and was designated "anti-BAFF monoclonal antibody (mAb)", using the variable region sequence available from the Protein Data Bank (ID no. 5Y9K) and an attenuated effector function activity IgG1 constant region, or was directly sourced (Benlysta; Myonex). WT TACI-Fc based on the atacicept sequence from sequence ID no. 54 from US patent no. 8,815,238-B2 was generated at Alpine Immune Sciences and designated "WT TACI 30-110-Fc". WT TACI-Fc based on the telitacicept sequence included with the World Health Organization (WHO) International Nonproprietary Names submission found in WHO Drug Information 2018, volume 32, issue no. 4 was generated at Alpine Immune Sciences and designated "WT TACI 13-118-Fc". Additionally, telitacicept was also directly sourced (Tai'ai; Clinigen).

Anti-APRIL mAb VIS649 (sibeprenlimab) was generated at Alpine Immune Sciences based on the sequence for sibeprenlimab included with the WHO International Nonproprietary Names submission found in WHO Drug Information 2020, volume 34, issue no. 4. Anti-APRIL mAb BION-1301 was generated at Alpine Immune Sciences based on sequence ID nos. 50 and 52 from US patent application US 2020/0079859-A1. Mouse BAFF-R (mBAFF-R) Fc fusion protein and anti–mouse APRIL (mAPRIL) mAb 4540 (13) were generated at Alpine Immune Sciences using a mouse Fc (mouse IgG1 D265A) with reduced effector function. Single-chain heterotrimeric APRIL and BAFF (comprising both the 2A:1B and 1A:2B forms) and a single-chain BAFF homotrimer were generated based on published sequences (28). Jurkat cells containing an NF-κB luciferase reporter were obtained from BPS Bioscience. A summary of all comparator reagents used in these studies is provided in Supplementary Table 1, available on the *Arthritis & Rheumatology* website at https://onlinelibrary.wiley.com/doi/10.1002/art.42462.

**Yeast surface display mutagenesis libraries and recombinant protein expression.** Yeast surface display libraries containing randomly mutated TACI variants (designated variable TNF receptor domains) were generated as described (29). Recombinant WT TACI and TACI variable TNF receptor domain–Fc fusion proteins were generated via transient expression in Expi293F cells (Thermo Fisher Scientific) per the manufacturer's instructions. Protein was purified from conditioned media harvests by capture and elution from protein A and formulated in 25 m*M* Tris, 161 m*M* arginine, pH 7.5. Material was tested for endotoxin levels (*Limulus* amebocyte lysate endotoxin kit; Charles River Laboratories), and all proteins contained <1 EU/mg.

**TACI/Jurkat/NF-κB reporter assay.** Jurkat/NF-κB cells were transduced with lentivirus to yield stable surface expression of human or mouse TACI (TACI/Jurkat/NF-κB), both of which demonstrate species cross-reactivity with APRIL and BAFF ligands. Recombinant human APRIL or BAFF (1–10 n*M*) were incubated with fixed or titrated (200 n*M*–2.5 p*M*) TACI domain–containing molecules or comparators. Ligands and inhibitors or Fc controls were incubated for 20 minutes by shaking at 150 revolutions per minute (rpm) at room temperature prior to the addition of $1.5 \times 10^5$ TACI/Jurkat/NF-κB cells per well within a white, 96-well, flat-bottom plate. Plates were incubated for 5 hours at 37°C, after which luciferase substrate solution (Bio-Glo Luciferase Assay System; Promega) was added while shaking at 150 rpm for 10 minutes. Relative luminescence units (RLU) were determined using a Cytation 3 (BioTek Instruments) or SpectraMax iD3 (Molecular Devices) imaging reader.

**Binding affinity measurement by surface plasmon resonance assay.** Affinity determination was conducted on a Biacore 3000 optical biosensor equipped with a CM5 sensor chip (GE) prepared with goat anti-human IgG capture antibody (Jackson ImmunoResearch). Povetacicept was captured to a level of 30 resonance units (RU) for the APRIL kinetic assays and 50 RU for the BAFF kinetic assays. Telitacicept was captured to a level of 135 RU for the APRIL kinetic assays and 145 RU for the BAFF kinetic assays. BAFF and APRIL concentrations (100 n*M*–0.137 n*M*) were prepared in HBS-EP running buffer (10 m*M* HEPES, pH 7.4, 150 m*M* NaCl, 3 m*M* EDTA, and 0.05% Surfactant P20). Association phases were monitored for 240 seconds at a flow rate of 30 μl/minute, and the dissociation phases for 400 seconds were captured at the same flow rate. A long dissociation experiment was run for the BAFF interactions using the 33.3 n*M* concentration for 1,800 seconds at a flow rate of 30 μl/minute. Data were aligned, double referenced, and fit using Scrubber software version 2.0 (Biologic Software).

**Human B cell differentiation assay.** CD19+ B cells were isolated from human peripheral blood mononuclear cells from 8 donors using negative selection kits (StemCell Technologies), activated with 2 n*M* recombinant human CD40L for 3 days, washed, and incubated another 4 days with 50 ng/ml recombinant human interleukin-21 plus 10 n*M* BAFF plus 10 n*M* APRIL. Supernatants were collected for serum immunoglobulin analysis and assayed using an immunoglobulin Milliplex kit (product no. HGAMMAG-301K; MilliporeSigma) with magnetic beads and antibodies specific for detecting soluble IgM, IgA, IgG1, IgG2, IgG3, and IgG4. Results were analyzed in GraphPad Prism version 9.0.2. For APRIL plus BAFF cultures, the percent inhibition of immunoglobulin secretion was determined using the following formula:

$$\frac{\text{median(APRIL + BAFF Ig value)} - \text{experimental Ig value}}{\text{median(APRIL + BAFF Ig value)}} \times 100$$

Cells were harvested, stained with Live/Dead Fixable Blue Dead Cell Stain kit (Invitrogen), anti-human IgM, anti-human IgD, anti-human CD27, anti-human CD38, and anti-human CD319 (BioLegend) and analyzed by flow cytometric analysis for B cell subset and plasma cell survival and differentiation. The gating strategy and exemplary contour plots for naive B cells, class-switched memory B cells, and plasma cells for each treatment condition are provided in Supplementary Figure 1, and a summary of the concentrations (ng/ml) of secreted immunoglobulin in the supernatants for each treatment condition is provided in Supplementary Table 2, available at https://onlinelibrary.wiley.com/doi/10.1002/art.42462.

**In vivo animal husbandry models ethics approval.** Mouse studies were approved by the Institutional Animal Care and Use Committee (IACUC) overseeing the vivarium where studies were conducted (Alpine Immune Sciences or Hooke Laboratories, Lawrence, Massachusetts), and followed the guidelines set forth in the 2011 Guide for the Care and Use of Laboratory Animals, Eighth Edition (National Research Council). The cynomolgus monkey study was conducted with approval from the Altasciences Preclinical IACUC (Everett, Washington).

**Mouse keyhole limpet hemocyanin (KLH) immunization model.** WT male, 10-week-old C57BL/6NJ mice (Jackson Laboratory) were randomly assigned into 5 groups (n = 5 per group). All mice except the naive control group were immunized with 250 μg KLH (product no. 374825-25MG; MilliporeSigma) in Dulbecco's phosphate buffered saline (Gibco–ThermoFisher Scientific) via intraperitoneal (IP) injection on day 0 and 12. Mice received either Fc control, povetacicept, WT TACI 30-110-Fc, or WT TACI 13-118-Fc by IP injection on days 4 and 11, molar matched to 15 mg/kg povetacicept. Mice were killed on day 20, and blood and spleens were collected for serum anti-KLH immunoglobulin analysis and splenocyte immunophenotyping.

**Mouse sheep red blood cell (SRBC) immunization model.** WT female, 8-week-old BALB/cJ mice (Jackson Laboratory) were randomly assigned into groups of 4 to 8 mice each. All but the naive control group were immunized with 25 µl of citrated sheep blood (Colorado Serum Company) via IP injection on day 0. Test articles were delivered via IP injection on days 1 and 6 and dosed for each study as indicated in the figure legends. Mouse anti-CD20 mAb (clone SA271G2) was obtained from BioLegend. Mice in each study were killed on day 15, and blood, spleen, and bone marrow were collected for serum anti-SRBC analysis and splenocyte and bone marrow immunophenotyping.

**Spontaneous lupus model in NZB/NZW mice.** Female 22-week-old (NZB × NZW)F1 mice (Jackson Laboratory) were randomized to 2 groups of 15 mice each based on their levels of serum anti–double-stranded DNA (anti-dsDNA) antibodies and proteinuria, and received either 17 mg/kg povetacicept or a molar-matched Fc control IP injection twice per week for 20 weeks until the end of the study at week 43. Body weight measurements were taken, and proteinuria measured weekly using urine dipsticks (Chemstrip 2 GP; Roche). Proteinuria was scored from 0 to 4, (0 = no detectable protein, 1 = <30 mg/dl, 2 = 30–100 mg/dl, 3 = 100–500 mg/dl, 4 = >500 mg/dl). Anti-dsDNA antibodies were measured throughout the study and at study end (week 43); serum levels of blood urea nitrogen were measured in final samples by IDEXX Laboratories. At 43 weeks of age (or earlier if mice became moribund during the study period), the left kidneys were collected in 10% neutral buffered formalin for hematoxylin and eosin or periodic acid–Schiff staining, and the right kidneys were embedded in OCT compound (Tissue-Tek; Sakura Finetek) and evaluated for IgG by immunohistochemistry. Stained sections were scored for glomerular IgG deposition (30). Submandibular glands were collected, weighed, fixed in 10% neutral buffered formalin for 48 hours, and embedded in paraffin blocks for histopathologic analysis of sialadenitis.

Data from flow cytometry analyses to evaluate immune cell subsets at study end (week 43) were not reliable enough to include in this article due to the lack of representative Fc control–treated mice surviving to study completion due to disease severity and the relatively low cell viability observed following overnight shipment of the spleens and lymph nodes. Of the samples that could be analyzed, the patterns of B cell reductions that were expected based on prior mouse model studies (e.g., reduced frequency of total B220+, transitional type 2, marginal zone, and follicular B cells) were observed in the povetacicept-treated group.

**Inducible model of lupus in bm12 mice.** Spleens and inguinal lymph nodes from 28 female, 8-week-old to 11-week-old I-A$^{bm12}$B6(C)-*H2-Ab1*$^{bm12}$/KhEgJ ("bm12") mice (Jackson Laboratory) were injected IP as single-cell suspensions into 26 WT female, 8-week-old to 9-week-old C57BL/6NJ recipient mice (Jackson Laboratory) (31) that had been randomly assigned to 2 groups on day 0. On day 5, test articles were delivered via IP injection and dosed as indicated in the figure legends, continuing twice per week until 6 days before mice were killed at the end of the study on day 95. Six female, age-matched, naive C57BL/6NJ mice were used as untreated controls. At study end, spleens were collected for flow cytometry, and the left kidney embedded in OCT compound as described above until evaluated for IgG staining by immunohistochemistry analysis.

**Flow cytometry analyses for mouse studies.** Spleens and bone marrow cells were processed into single-cell suspensions, and red blood cells were lysed with 1× red blood cell lysis buffer (BioLegend) per the manufacturer's instructions before cells were counted. Live cells ($1 \times 10^6$) were then stained with antibodies listed in Supplementary Table 3 (https://onlinelibrary.wiley.com/doi/10.1002/art.42462) for flow cytometry analysis of immune cell subsets following staining with Live/Dead Fixable Aqua or Live/Dead Fixable Blue Dead Cell Stain kits (Life Technologies Corp) diluted 1:1,000 in Dulbecco's phosphate buffered saline and pre-incubation with Mouse BD Fc Block (BD Biosciences). Stained cells were collected on an LSRII (BD Biosciences) or CytoFLEX LX (Beckman Coulter) flow cytometer. Flow cytometry gating examples are provided in Supplementary Figures 2–3 (https://onlinelibrary.wiley.com/doi/10.1002/art.42462). Data were analyzed using FlowJo software versions 10.7.2 and 10.8.1 and graphed using GraphPad Prism software.

**Non-human primate pharmacokinetics/pharmacodynamics study.** Povetacicept and WT TACI 13-118-Fc (9 mg/kg each) were evaluated after a single, 30-minute intravenous infusion on day 0 to 2 female cynomolgus monkeys per group. Control animals received vehicle (25 m*M* Tris, 161 m*M* arginine, pH 7.5) under the same conditions. Blood was collected before infusion and at various time points (0.083, 2, 6, 24, 72, 144, 312, 480, 624, 816, and 984 hours after infusion) through day 26 to characterize test article serum concentrations, while blood sampling continued through day 42 to assess serum concentrations of IgM, IgA, and IgG. Noncompartmental analysis was conducted, and pharmacokinetic parameters were estimated using Phoenix WinNonlin software (Certara). Serum IgM, IgA, and IgG were measured by Altasciences as part of a standard serum chemistry panel of analytes.

**Statistical analysis.** Statistically significant differences between groups were determined using one-way analysis of variance (ANOVA) and uncorrected Fisher's least significant difference multiple comparison test (KLH model, SRBC IgM, IgG1, IgG2a, and IgG2b data, plasma cell and plasmablast data, and follicular helper T cell data); Kruskal-Wallis test and uncorrected Dunn's test (human B cell assay, SRBC IgG2b and IgM data,

germinal center and follicular helper T cell data, the bm12 model, and plasma cell data); unpaired 2-tailed Mann-Whitney test (data for single time points in the NZB/NZW model); two-way repeated measures ANOVA (data over time in the NZB/NZW model); or Mantel-Cox log rank test (survival analysis in the NZB/NZW model). Normality testing was performed to select the appropriate statistical method. The naive groups in the KLH, SRBC, and bm12 models were not included in the statistical analyses. No animals were excluded from analysis in any in vivo model. GraphPad Prism version 9.0.2 was used for statistical analyses, and *P* values less than 0.05 were considered statistically significant for all tests.

## RESULTS

**Engineering and characterization of an optimized APRIL and BAFF inhibitor.** The extracellular domain of TACI consists of 2 TNF receptor cysteine-rich domains (CRDs) and a stalk region (Supplementary Figure 4A, https://onlinelibrary.wiley.com/doi/10.1002/art.42462). APRIL and BAFF binding sites on TACI are located within CRD2 (32). Therefore, the single TACI CRD2 domain was selected for further optimization using a directed engineering approach to enhance binding of TACI CRD2 to APRIL and BAFF. Libraries containing mutagenized TACI CRD2 were generated via error-prone polymerase chain reaction and selected for enhanced APRIL and BAFF binding through yeast surface display (29) (Supplementary Figures 5A and 5B). Selected TACI variant TNF receptor domain hits were fused to a human IgG1 Fc lacking effector function (33), expressed in mammalian cells and evaluated in the TACI/Jurkat/NF-κB reporter assay (Supplementary Figure 5C). The highest-ranking candidate, TACI variant TNF receptor domain H88-Fc, was designated ALPN-303 (povetacicept). The inhibitory activity of povetacicept in the TACI/Jurkat/NF-κB assay was approximately 19-fold and 14-fold greater than WT TACI 13-118-Fc for neutralization of APRIL or BAFF, respectively (Figure 1A and Supplementary Table 4).

Povetacicept has 3 amino acid substitutions within TACI CRD2 (K77E, F78Y, and Y102D), all 3 of which appear necessary for optimal activity because all single- and double-substitution revertant-containing versions exhibited decreased inhibitory activity relative to povetacicept (data not shown). By surface plasmon resonance, the affinity of povetacicept for BAFF was 59.3 p*M* and ∼8-fold better than that of telitacicept (491 p*M*); povetacicept's affinity for APRIL was ∼1 p*M*, while telitacicept's affinity for APRIL was not able to be determined due to multiple on and off rates (Figures 1B and 1C).

**More potent inhibition of APRIL and BAFF by povetacicept than comparator molecules in vitro.** The ability of povetacicept to inhibit APRIL and BAFF activity alone or in combination was measured in the TACI/Jurkat/NF-κB reporter assay relative to comparator APRIL and/or BAFF inhibitors including telitacicept, the anti-BAFF antibody belimumab, and an anti-APRIL mAb derived from the published sequence for BION-1301 (12) (Supplementary Table 4, https://onlinelibrary.wiley.com/doi/10.1002/art.42462). Povetacicept effectively neutralized APRIL 5.7-fold better than the anti-APRIL mAb, and neutralized BAFF 3.4-fold better than belimumab (Figure 2A, Supplementary Table 4). Povetacicept was also the most potent inhibitor of the combination of APRIL and BAFF, with a >50-fold lower median inhibition concentration ($IC_{50}$) value relative to telitacicept, and a 3.5-fold better $IC_{50}$ value relative to the combination of anti-APRIL mAb plus belimumab (Figure 2A, Supplementary Table 4).

APRIL and BAFF can form heterotrimeric proteins at a 2:1 ratio (5,6). Additionally, soluble BAFF exists in a high molecular weight complex designated as BAFF 60-mer (4). Inhibition of APRIL and BAFF trimers/heterotrimers as well as BAFF 60-mer is likely required for full inhibition of these pathways in autoimmune settings where multiple forms of these ligands can be present or elevated (4). Povetacicept was tested for its ability to inhibit BAFF 60-mer–induced and APRIL/BAFF heterotrimer–induced signaling in the TACI/Jurkat/NF-κB assay. Povetacicept inhibited BAFF 60-mer significantly better ($P < 0.0001$) than the full-length WT TACI-Fc proteins tested (Supplementary Figures 6A and 6E). In addition, single-chain heterotrimers of APRIL and BAFF were generated, consisting of BAFF-APRIL-APRIL and APRIL-APRIL-BAFF formats to represent both possible forms (28). A single-chain BAFF homotrimer was included as a control. Povetacicept demonstrated greater inhibition against the BAFF homotrimer and BAFF/APRIL heterotrimers compared to telitacicept (Supplementary Figures 6B–E). An anti-APRIL antibody produced from the published sequence for VIS649 (sibeprenlimab) only inhibited the BAFF-APRIL-APRIL heterotrimer, while belimumab inhibited the APRIL-APRIL-BAFF heterotrimer (in contrast to previously published results [28]) and the BAFF homotrimer. Collectively, these findings indicate that directed engineering of a single TACI CRD2 domain is sufficient to generate significantly enhanced affinity for APRIL and increased BAFF affinity, resulting in inhibitory activity superior to clinically relevant therapeutics, including monoclonal antibodies.

**More potent inhibition of class-switched memory B cell and plasma cell survival and immunoglobulin secretion than telitacicept, anti-APRIL, or anti-BAFF in primary human B cell assays.** We next evaluated the ability of povetacicept to affect primary human B cell proliferation, differentiation, and immunoglobulin secretion in vitro. Purified human pan B cells were first stimulated for 3 days with recombinant CD40L and then plated for 4 days in the presence of exogenous BAFF, APRIL, and test articles. Compared to telitacicept, anti-APRIL mAb, or anti-BAFF mAb, povetacicept more potently inhibited expansion of total B cells and various key B cell subsets, including class-switched memory B cells and plasma cells (Figure 2B and Supplementary Figure 1, https://onlinelibrary.wiley.

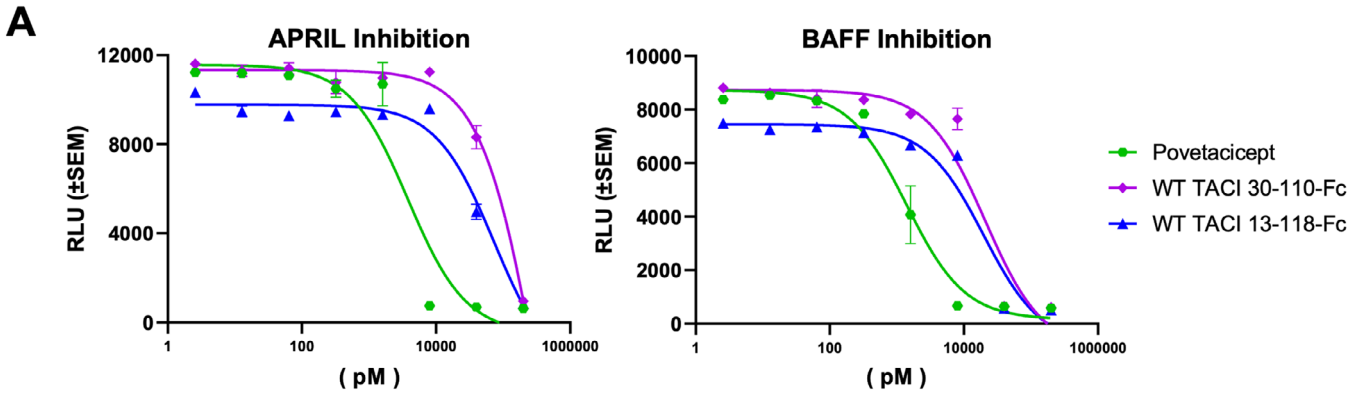


B

| Test Article | Sample | $k_{a\ app}$ 1x10$^9$ ($M^{-1}s^{-1}$) | $k_{d\ app}$ 1x10$^{-3}$ ($s^{-1}$) | $R_{max}$ (RU) | $K_{D\ app}$ (pM) |
|---|---|---|---|---|---|
| Povetacicept | APRIL | 7.0 ± 7 | 7.0 ± 6 | 55.5 ± 0.1 | 1.00 ± 0.04 |
| Telitacicept | APRIL | CNBD* | CNBD | CNBD | CNBD |

| Test Article | Sample | $k_a$ 1x10$^5$ ($M^{-1}s^{-1}$) | $k_d$ 1x10$^{-5}$ ($s^{-1}$) | $R_{max}$ (RU) | $K_D$ (pM) |
|---|---|---|---|---|---|
| Povetacicept | BAFF | 6.19 ± 0.01 | 3.67 ± 0.02 | 52.8 ± 0.3 | 59.3 ± 0.1 |
| Telitacicept | BAFF | 1.75 ± 0.01 | 8.63 ± 0.02 | 47.6 ± 0.4 | 491 ± 1 |

**CNBD – could not be determined*

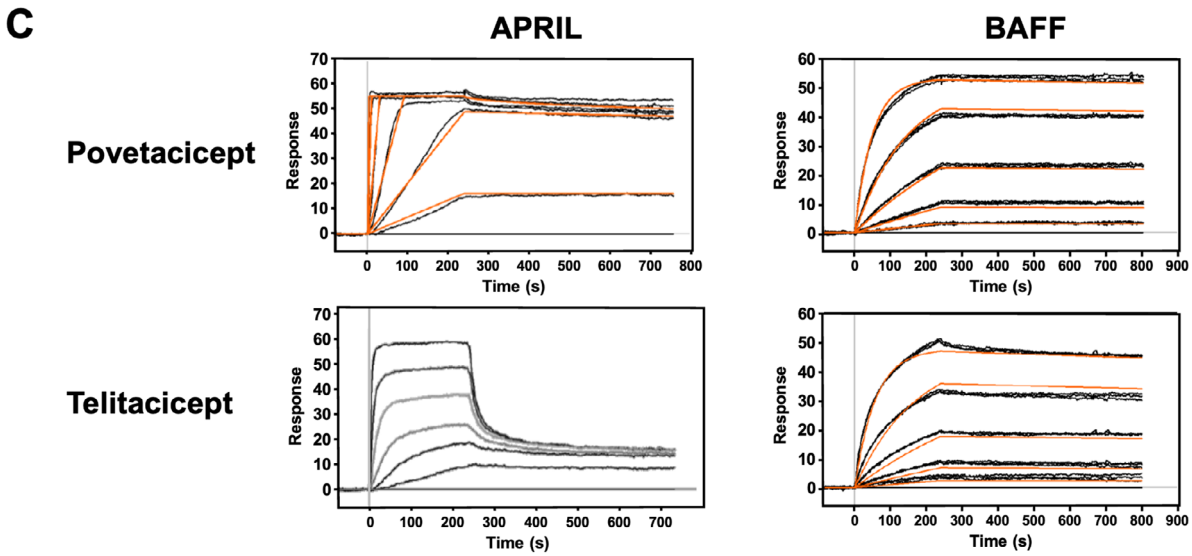


**Figure 1.** Assessment of APRIL and BAFF inhibitory activity and binding by various TACI-Fc fusion proteins and the affinity-optimized TACI variant povetacicept. **A**, APRIL and BAFF inhibition by TACI variants and povetacicept evaluated in the TACI/Jurkat/NF-κB reporter assay. Increased inhibitory activity is indicated by reduced luciferase production. **B**, Affinity measurements of povetacicept and telitacicept binding to recombinant human APRIL and BAFF as determined by surface plasmon resonance (SPR). **C**, SPR sensorgrams with povetacicept and telitacicept at medium density shown in black lines and results from nonlinear least squares regression analysis of the data shown in orange lines. Telitacicept was sourced from Clinigen. Analyte concentrations were prepared in running buffer, ranging from 33.3 n*M* to 0.137 n*M* for APRIL and 33.3 n*M* to 0.412 n*M* for BAFF in 3-fold serial dilution steps. WT = wild-type; RLU = relative luminescence units; RU = resonance units.

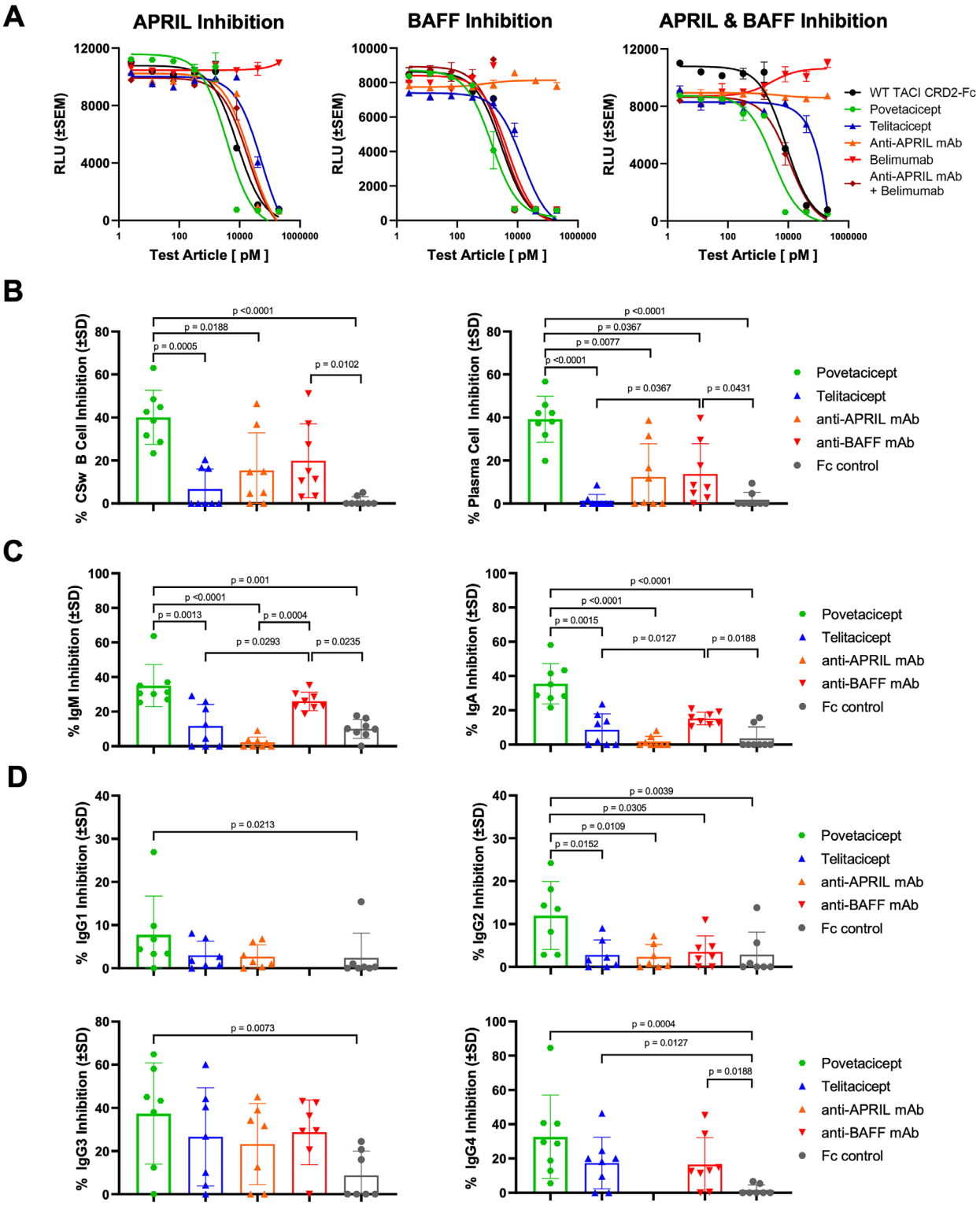


**Figure 2.** Povetacicept inhibits APRIL and BAFF more potently than comparator molecules. **A**, APRIL, BAFF, or APRIL plus BAFF inhibition by povetacicept and comparator molecules was evaluated in the TACI/Jurkat/NF-κB reporter assay. **B**, CD19+ B cells were activated with recombinant human CD40L and recultured with exogenous APRIL, BAFF, and povetacicept, or the indicated comparator molecules. Cells were stained and analyzed by flow cytometry to identify class-switched (CSw) memory B cells (IgD, IgM, CD27+) or plasma cells (IgM, IgD, CD38+, CD319+). **C** and **D**, CD19+ B cells were activated as in **B**. After 7 days, supernatants were collected and IgM, IgA (**C**), IgG1, IgG2, IgG3, and IgG4 (**D**) secretion was quantitated by multiplex analysis. Telitacicept was sourced from Clinigen, and belimumab from Myonex. Bar charts show the mean ± SD. Statistically significant differences between group median values were determined using Kruskal-Wallis test and uncorrected Dunn's test. *P* values less than 0.05 were considered statistically significant. mAB = monoclonal antibody. See Figure 1 for other definitions.

com/doi/10.1002/art.42462). Povetacicept's potent inhibition of B cell expansion and survival was also correlated with significant reductions in immunoglobulins secreted into the culture media (Figures 2C and 2D and Supplementary Table 2). These findings were consistent with the ability of povetacicept to inhibit the differentiation of naive B cells to plasma cells, with activity superior to anti-BAFF or anti-APRIL mAb, confirming that coinhibition of both APRIL and BAFF results in greater suppression of immunoglobulin secretion compared to blockade of either cytokine alone. In addition, povetacicept demonstrated superior activity compared to telitacicept in this assay, consistent with its improved affinity for APRIL and BAFF.

**More potent inhibition of APRIL and BAFF by povetacicept than comparator molecules in mouse immunization models.** To determine if the enhanced APRIL and BAFF blockade observed with povetacicept in vitro translated into enhanced activity in vivo, povetacicept was evaluated in a mouse KLH immunization model. Notably, povetacicept and comparators inhibited mouse and human APRIL and BAFF with comparable relative $IC_{50}$ values (Supplementary Table 4, https://onlinelibrary.wiley.com/doi/10.1002/art.42462). Mice were challenged with KLH as a model antigen and then treated with povetacicept or WT TACI-Fc comparators to assess their immunomodulatory activity. KLH immunization increased spleen size and cellularity as shown by the significant increase in splenocyte numbers in the Fc control–treated group compared to the naive group (Figure 3A and Supplementary Figure 7A). Mice treated with povetacicept on days 4 and 11 following KLH immunization on day 0 had significantly reduced total spleen cellularity at the end of the study (day 20) compared to mice treated with Fc control, WT TACI 30-110-Fc, or WT TACI 13-118-Fc (Figure 3A and Supplementary Figure 7A). Except for the least mature transitional type 1 B cells, all splenic B cell subsets evaluated (gated as defined in Supplementary Figures 2–3), including transitional type 2, follicular, marginal zone, germinal center, and plasma cells were significantly reduced following povetacicept treatment, exceeding the activity of WT TACI-Fc (Figures 3A and 3B and Supplementary Figure 7A).

There was no significant effect on the number of splenic T cells with povetacicept, WT TACI 30-110-Fc, or WT TACI 13-118-Fc treatment (Supplementary Figure 7B). In contrast, the total number of CD4+ follicular helper T cells per spleen was significantly lower in each of the treatment groups compared to the Fc control group, with povetacicept treatment mediating the greatest reductions (Figure 3C). Povetacicept also significantly reduced the formation of anti-KLH IgM and IgG1 antibodies at day 20, reflecting its impact on a primary humoral immune response (Figure 3D). The reductions in the anti-KLH immunoglobulin concentrations observed with povetacicept treatment were significantly greater than those observed with WT TACI-Fc treatment.

Povetacicept was also evaluated for its impact on the antibody response to another T cell–dependent antigen in a primary SRBC immunization model. Following SRBC immunization, mice were dosed twice with Fc control, povetacicept, telitacicept, an anti-mAPRIL mAb, mBAFF-R-Fc, or a combination of anti-mAPRIL plus mBAFF-R-Fc. Mice were killed on day 15, and spleens and bone marrow were processed for immunophenotyping by flow cytometry. Serum titers of anti-SRBC IgM and IgG were also measured. Povetacicept demonstrated significantly enhanced immunosuppressive activity over all of the comparators, including the combination of anti-mAPRIL plus mBAFF-R-Fc, for most of the end points, including reduced anti-SRBC immunoglobulin responses (Figure 4A), decreased numbers of splenic germinal center B cells (Figure 4B), follicular helper T cells (Figure 4C), plasma cells (Figure 4D), and plasmablasts (Figure 4E), as well as reductions in the percentages of long-lived plasma cells (Figure 4F) and total plasma cells in the bone marrow (Figure 4G).

Similar SRBC immunization studies were conducted to compare the activity of povetacicept to telitacicept and a depleting mouse anti-CD20 antibody. Povetacicept again demonstrated enhanced immunosuppressive activity over WT TACI CRD2-Fc, telitacicept, and anti-CD20, as determined by end points similar to those listed above (Supplementary Figure 8, https://onlinelibrary.wiley.com/doi/10.1002/art.42462). Collectively, the results from these immunization studies demonstrate that the optimized dual inhibition of APRIL and BAFF by povetacicept provides deeper and more sustained ASC and B cell suppression compared to anti-CD20, telitacicept, inhibitors of either APRIL or BAFF alone, or a combination of APRIL and BAFF inhibitors, leading to greater suppression of T cell–dependent antibody responses.

**Disease suppression by povetacicept in spontaneous and inducible models of SLE.** Povetacicept was next evaluated in the NZB/NZW spontaneous mouse model of lupus. In this model, NZB mice are bred to NZW mice, and by 6 months of age mice develop severe lupus-like features similar to those of human lupus patients. The model is characterized by the presence of serum antinuclear autoantibodies (including anti-dsDNA), mild vasculitis, and the development of immune complex–mediated glomerulonephritis (34). In this study, 22-week-old NZB/NZW mice were randomized based on serum anti-dsDNA antibody titers and proteinuria and treated twice weekly with povetacicept or an Fc control for up to 20 weeks. Compared to treatment with Fc control, povetacicept treatment provided protection from disease, including reduced proteinuria and development of anti-dsDNA IgG autoantibodies (Figures 5A and 5B). Moreover, povetacicept treatment significantly improved survival, suppressed blood

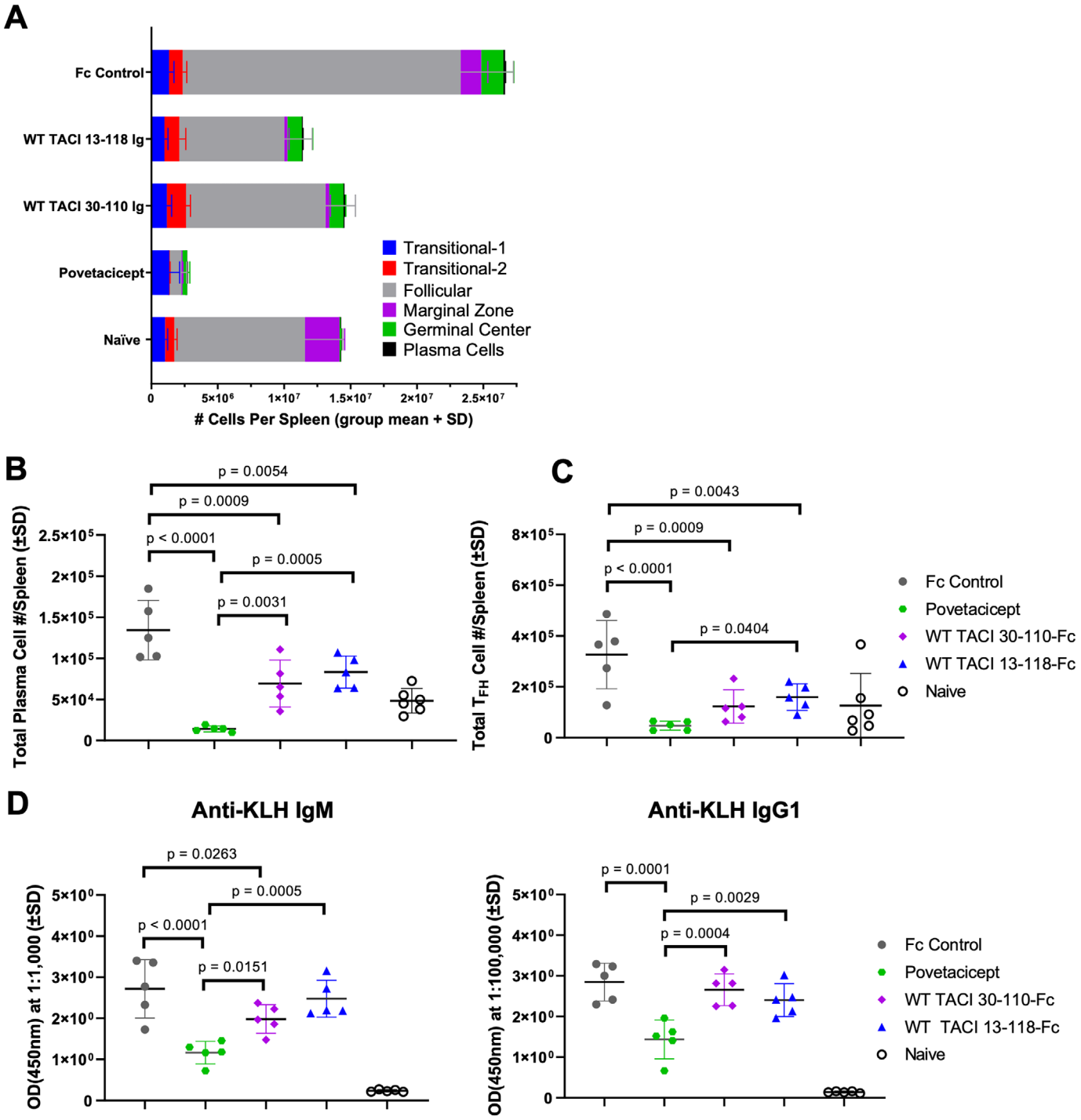


**Figure 3.** Povetacicept reduces splenic immune cell subsets and inhibits T cell–dependent antibody formation more potently than telitacicept in keyhole limpet hemocyanin (KLH)–immunized mice. C57BL/6NJ mice were challenged with KLH on days 0 and 12 and dosed intraperitoneally with povetacicept, Fc control, or WT TACI-Fc comparators (molar-matched to 10 mg/kg povetacicept) on days 4 and 11. **A**, Splenic B cell subsets (total number of cells/spleen) from KLH-challenged or naive mice at day 20 determined by flow cytometry. Individual data plots for B cell subsets and T cells are presented in Supplementary Figure 2 (https://onlinelibrary.wiley.com/doi/10.1002/art.42462). **B** and **C**, Total number of plasma cells (**B**) and follicular helper T cells (**C**) per spleen from KLH-challenged or naive mice at day 20 were enumerated by flow cytometry. **D**, Day 20 serum samples were analyzed for KLH-specific IgM or IgG1. Symbols represent individual mice. Lines with whiskers show the mean ± SD. WT = wild-type; OD = optical density.

urea nitrogen, reduced histopathologic scores for sialadenitis, and reduced glomerulonephritis and deposition of renal IgG (Figures 5C–H).

Povetacicept was also evaluated in the bm12 inducible model, in which lupus-like disease was induced by injecting C57BL/6NJ mice with major histocompatibility complex–mismatched bm12

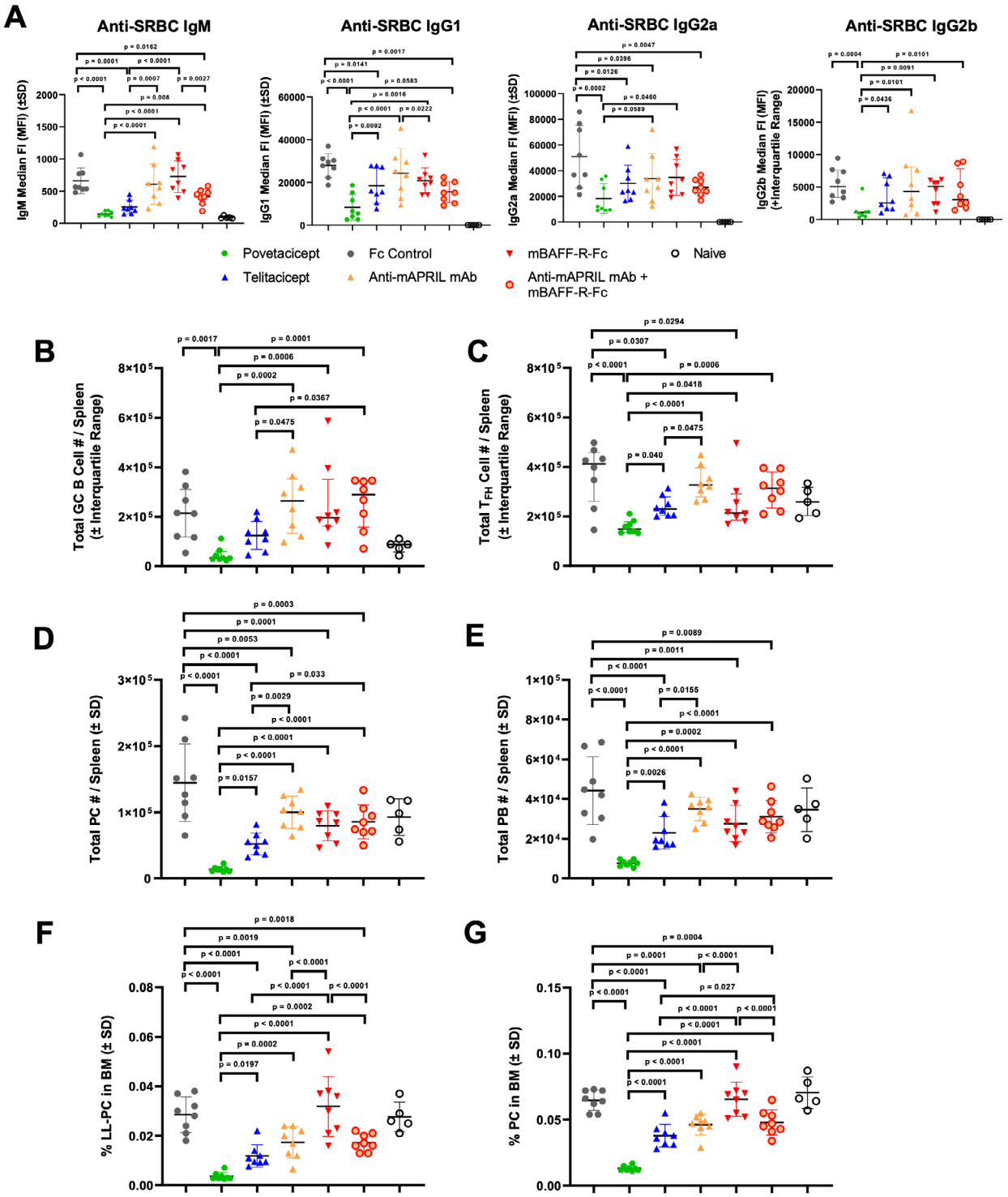


**Figure 4.** Povetacicept demonstrates enhanced immunosuppressive activity over telitacicept and BAFF- or APRIL-only inhibitors in a mouse sheep red blood cell (SRBC) immunization model. Following SRBC immunization on day 0, female BALB/cJ mice were dosed intraperitoneally on days 1 and 6 with 10 mg/kg povetacicept, Fc control, telitacicept, anti–mouse APRIL (mAPRIL) mAb, mouse BAFF receptor (BAFF-R)–Fc, or a combination of 10 mg/kg each anti-mAPRIL mAb plus mBAFF-R-Fc. **A–E**, Anti-SRBC Ig concentrations in serum were measured on day 15 (**A**), and the total number of germinal center (GC) B cells (**B**), CD4+ follicular helper T (Tfh) cells (**C**), plasma cells (PCs) (**D**), and plasmablasts (PBs) (**E**) per spleen were enumerated by flow cytometry. **F** and **G**, The percentage of viable long-lived plasma cells (LL-PCs; defined as TACI$^{high}$CD138$^{high}$B220–CD19–) (**F**) and total plasma cells (TACI$^{high}$CD138$^{high}$ cells) (**G**) in the bone marrow (BM) were also determined by flow cytometry. Symbols represent individual mice. Lines with whiskers show the mean ± SD (**A**,**D–G**) or median ± interquartile range (IgG2b data in **A** and **B–C**). Statistically significant differences between groups were determined using one-way analysis of variance and uncorrected Fisher's least significant difference multiple comparison test (**A**,**D–G**) or Kruskal-Wallis test and uncorrected Dunn's test (IgG2b data in **A** and **B–C**). MFI = median fluorescence intensity.

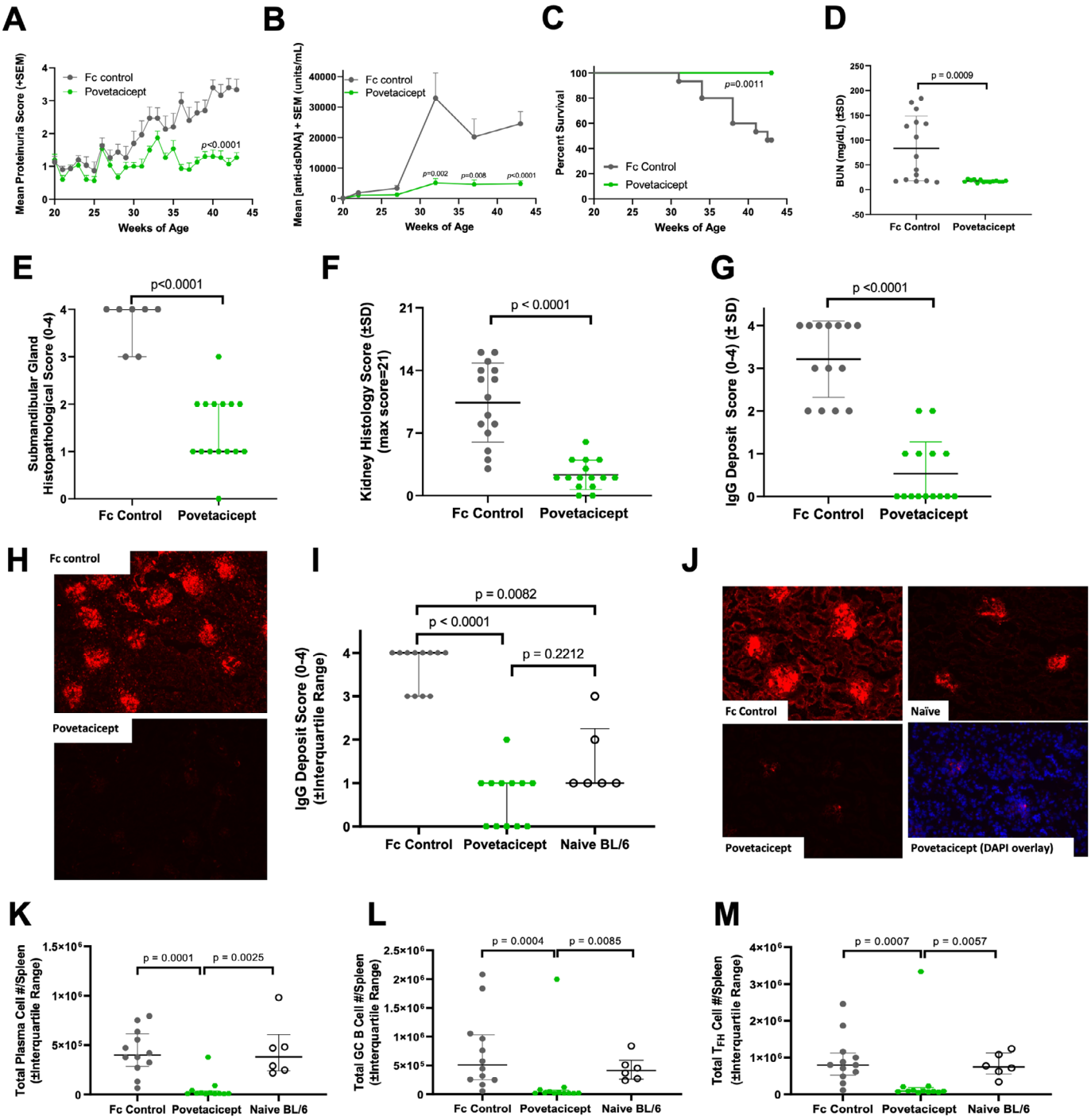


**Figure 5.** Povetacicept suppresses disease in systemic lupus erythematosus mouse models. NZB/NZW F1 mice received 17 mg/kg povetacicept or molar-matched Fc control intraperitoneally (IP) every 3–4 days from 22–42 weeks of life for 40 total doses. **A–C**, Mean ± SEM proteinuria scores (**A**) and anti–double-stranded DNA (anti-dsDNA) IgG levels (**B**), and survival over time (**C**) in mice treated with povetacicept versus Fc control. **D–H**, Serum blood urea nitrogen (BUN) level (**D**), submandibular gland histopathologic score (**E**), and kidney histology score as a sum of total glomerular, tubular, and interstitial lesions from left kidney (**F**) and renal IgG deposit score evaluated by immunohistochemistry (IHC) from right kidney (**G**) at study end (week 43), with representative IHC images (10×) of renal IgG deposits from an Fc control– or povetacicept-treated mouse (**H**). **I–M**, C57BL/6NJ mice were injected IP with bm12 splenocytes on day 0 then dosed IP twice per week days 5–88 (6 days prior to study end on day 95) with 10 mg/kg povetacicept or molar-matched Fc control. Age-matched naive mice were controls. Renal IgG deposit score was evaluated by IHC for each mouse from left kidney at study end (**I**), with representative IHC images (20×) of renal IgG deposits from Fc control, povetacicept, or naive mouse (**J**). Total plasma cells (**K**), GC B cells (**L**), and CD4+ Tfh cells (**M**) per spleen were enumerated by flow cytometry. In **D–M**, symbols represent individual mice. Lines with whiskers are the mean ± SD (**D**,**F**,**G**) or median ± interquartile range (**E**,**I**,**K–M**). See Figure 4 for other definitions.

splenocytes. Glomerular IgG immune deposits were evident by ~4 weeks following splenocyte transfer. Mice were treated with povetacicept or an Fc control twice weekly from days 5 to 88. Glomerular IgG deposits were significantly elevated in this model at the end of the study (day 95), and povetacicept significantly reduced these deposits compared to Fc control (Figures 5I and 5J). Furthermore, povetacicept treatment resulted in significantly lower numbers of splenic plasma cells, germinal center B cells, and follicular helper T cells (Figures 5K–M) compared to Fc control, similar to what was observed in the KLH and SRBC immunization models.

**Suppression of serum immunoglobulin by povetacicept in cynomolgus monkeys.** A pharmacokinetics/pharmacodynamics study in cynomolgus monkeys was conducted to evaluate povetacicept relative to WT TACI 13-118-Fc, both administered at a single 9 mg/kg intravenous dose. Dose-normalized serum concentrations of the test articles and serum IgM, IgA, and IgG levels are shown in Figure 6A; published atacicept pharmacokinetic data (35) are overlaid for comparison, based on a 1 mg/kg intravenous administration to cynomolgus monkeys. Both test articles were well-tolerated, and serum concentrations of povetacicept and WT TACI 13-118-Fc were measurable to day 26 postinfusion. Time to maximum concentration was assessed from the first collection time point following the end of infusion (0.083 hours postinfusion) for both test articles. Exposure was similar between the 2 test articles based on the maximum serum concentration. However, based on the area under the curve from time 0 to the last time t, exposure was

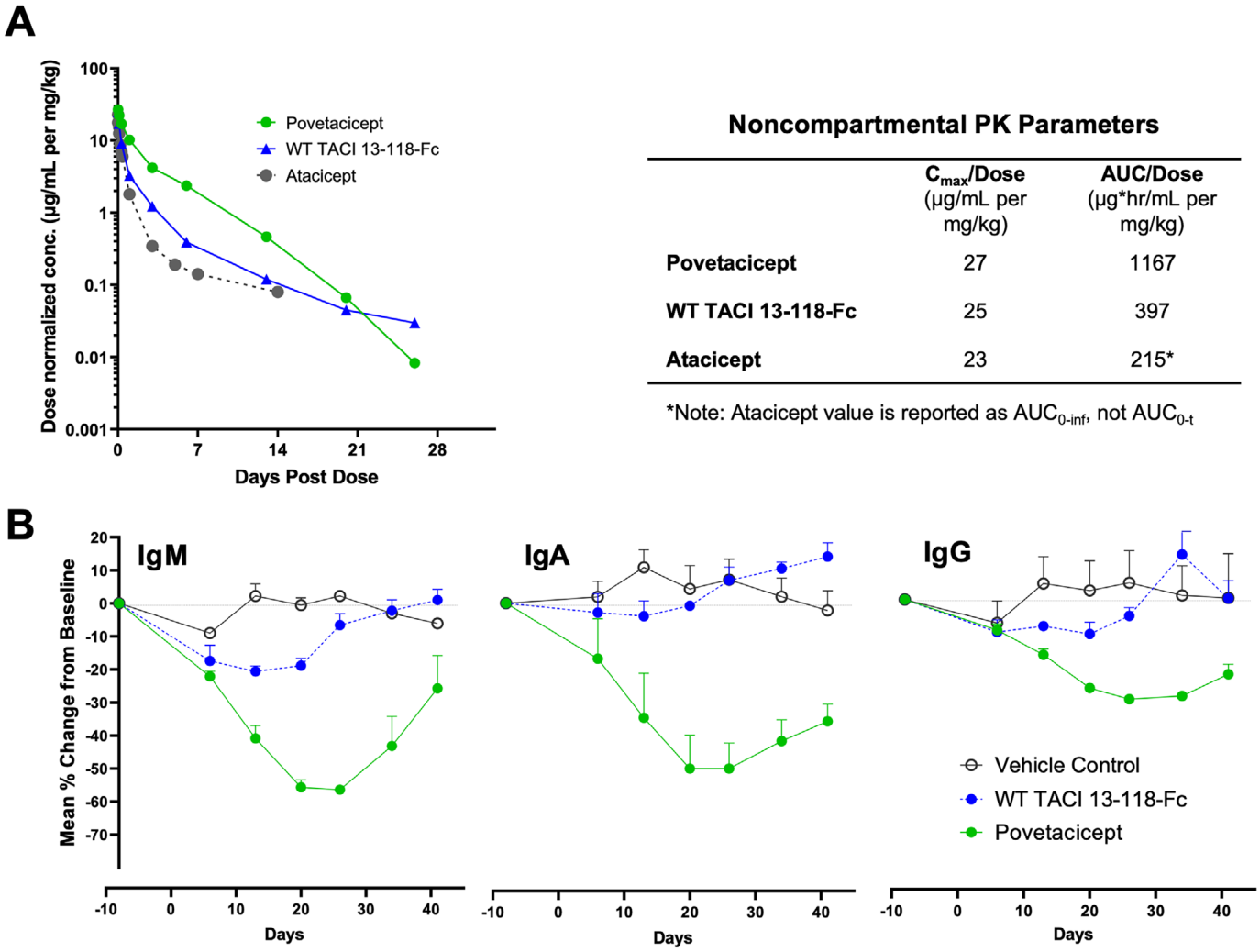


**Noncompartmental PK Parameters**

| | $C_{max}$/Dose (µg/mL per mg/kg) | AUC/Dose (µg*hr/mL per mg/kg) |
|---|---|---|
| **Povetacicept** | 27 | 1167 |
| **WT TACI 13-118-Fc** | 25 | 397 |
| **Atacicept** | 23 | 215* |

*Note: Atacicept value is reported as $AUC_{0\text{-}inf}$, not $AUC_{0\text{-}t}$

**Figure 6.** Povetacicept exhibits increased exposure and enhanced Ig suppression versus wild-type (WT) TACI 13-118-Fc in non-human primates. Female cynomolgus monkeys (2 per treatment group) were administered a single 30-minute intravenous (IV) infusion on day 0 of vehicle (0 mg/kg) or 9 mg/kg povetacicept or WT TACI 13-118-Fc. Serum was collected at various time points (before infusion and at 0.083, 2, 6, 24, 72, 144, 312, 480, 624, 816, and 984 hours postinfusion), and samples were analyzed for test article concentrations using enzyme-linked immunosorbent assay (ELISA). **A**, Dose-normalized concentration curves are shown. Atacicept pharmacokinetic (PK) data from a 1 mg/kg IV administration were obtained from a previous publication (ref. 35). **B**, Mean percentage change from baseline (8 days before infusion) of serum concentrations of IgM, IgA, and IgG in each treatment group measured by ELISA at various time points. Whiskers show the upper range. $C_{max}$ = maximum concentration; AUC = area under the curve.

3 to 4 times higher after povetacicept dosing compared to WT TACI 13-118-Fc. The dose-normalized maximum serum concentration values were 27, 25, and 23 μg/ml per mg/kg, and the dose-normalized area under the curve values were 1,167, 397, and 215 μg × hour/ml per mg/kg for povetacicept, WT TACI 13-118-Fc, and atacicept, respectively.

The levels of serum IgM, IgA, and IgG in animals receiving povetacicept decreased an average of ∼60%, ∼50%, and ∼30% at their nadir on day 27, respectively, compared to pre-dose levels (Figure 6B). In comparison, the serum immunoglobulin decreases from baseline in animals treated with WT TACI 13-118-Fc versus pre-dose levels were much less dramatic (∼20% decrease in IgM, no apparent change in IgA, and ∼15% reduction in IgG).

## DISCUSSION

SLE and other autoantibody-related rheumatic diseases continue to have high unmet need for treatment options. In SLE, development of treatment options has been hindered by complex pathogenesis and heterogeneity of disease, suggesting that multiple pathways or aspects of B cell development and differentiation may require simultaneous inhibition to enable durable treatment response. While B cell–depleting agents such as rituximab/ocrelizumab/obinutuzumab (anti-CD20) and obexelimab (anti-CD19) have exhibited favorable clinical effects in certain autoimmune disease settings, this has not translated to SLE, in which rituximab failed to demonstrate benefit in SLE and LN trials (36,37). One possible limitation of these therapeutics is that CD20 and CD19 are not expressed on all ASCs or long-lived plasma cells, and only earlier-stage B cells (including pro/pre, immature, mature, and memory B cells) are depleted, sparing most pathogenic plasmablasts and plasma cells (38).

Targeting or cotargeting BAFF and/or APRIL has garnered increasing interest as an alternative to antibody-dependent cell-mediated cytotoxicity–mediated B cell depletion. Preclinical studies have demonstrated that starving B cells of these 2 critical B cell survival and differentiation factors can significantly reduce all B cell subsets beyond the immature type 1 stage of development, including long-lived plasma cells, without affecting CD19+CD20+ pro/pre B cell precursors (39). Inhibition of ASCs can dramatically impact pathogenic antibody production and thereby potentially reduce disease activity. Although early efforts to target the BAFF/APRIL pathway focused on agents like belimumab that neutralize only BAFF, a preponderance of preclinical data suggest that inhibition of both APRIL and BAFF is required to impact survival of more differentiated, pathogenic TACI+BCMA+ASCs (3).

APRIL has a particularly important role in IgA class switching, production, and glycosylation, as first indicated by studies of APRIL knockout mice (40). In addition, elevated plasma APRIL levels in IgA nephropathy patients are associated with more severe clinical manifestations such as high proteinuria and galactose-deficient IgA1 levels (41), which are important causal factors and contribute to disease pathogenesis. Indeed, early trials of BION-1301 and sibeprenlimab suggest that APRIL-only inhibition can mediate significant decreases in immunoglobulin (particularly IgA) in healthy individuals, and BION-1301 impacts proteinuria in IgA nephropathy patients in an ongoing trial (42). However, targeting APRIL alone has its own limitations and would not be expected to impact less mature BAFF-dependent B cells that can also contribute to disease pathogenesis (38). BAFF neutralization leads to down-regulation of B cell function, decreases in autoantibody production, and inhibition of tertiary lymphoid structure formation in the kidney (3).

Belimumab was the first approved therapy for SLE and LN after a 50-year drought (38), underscoring the need for new therapies. Another development in SLE therapy was the recent approval of anifrolumab, an anti–type I interferon (IFN) receptor antibody (43,44). Anifrolumab targets a distinct pathophysiology of SLE from B cell modulators by targeting myeloid dendritic cells rather than B cells, although type I IFNs are known to indirectly promote B cell differentiation and loss of tolerance. IFN-regulated gene expression is significantly increased in SLE; however, IFN gene signature expression has not been predictive of response, underscoring the pleiotropic effects of the IFN system (43). In contrast, the presence of high serum levels of BAFF and APRIL in patients with SLE is well established and has been described in numerous studies (3). High serum BAFF levels have also been correlated with elevated autoantibody levels, particularly anti-dsDNA antibodies (3).

Until now, cotargeting BAFF and APRIL has been attempted only with development of the WT TACI-Fc molecules atacicept and telitacicept, though the affinity of WT TACI-Fc for APRIL is arguably suboptimal, well below that achieved by anti-APRIL mAb, which range in affinity from $K_d$ = 0.95 p*M* to $K_d$ = 400 p*M*, depending on the method used (Figure 1) (12,13). Thus, while these molecules arguably neutralize BAFF sufficiently, their inefficient blockade of APRIL activity leaves clear room for improvement. Reports of affinity-enhanced soluble BCMA fusion proteins as an alternate approach to cotarget APRIL and BAFF were recently described and may be in preclinical development, though their structure and mutational burden have not yet been revealed (45,46). Povetacicept addresses the limitations of WT TACI-Fc by dramatically improving the affinity of TACI for both APRIL and BAFF (Figure 1), leading to functional neutralizing activity both in vitro (Figure 2) and in vivo (Figures 3–5). Moreover, a single dose of povetacicept led to notably enhanced suppression of serum immunoglobulins relative to WT TACI 13-118-Fc in a non-human primate study (Figure 6). The higher serum exposures and more potent immunomodulatory activities observed with povetacicept may enable improved efficacy, lower clinical doses, and/or longer dosing intervals compared to other TACI-Fc molecules. For example, whereas telitacicept is generally dosed once per week, povetacicept is anticipated to be

administered once at least every 4 weeks, based on exposure and pharmacodynamic observations.

A theoretical safety concern regarding povetacicept's highly potent inhibition of BAFF and APRIL is infection, especially considering prior reports of increased infection risk with agents such as rituximab (47–49) or atacicept (50). However, such findings may have been confounded by the use of prior concomitant immunosuppressive medications and/or inadequate safety monitoring, such as of circulating immunoglobulin levels (51). Indeed, the most recently studied drug in this class in SLE, telitacicept, appears to be well tolerated so far without a clear imbalance in infectious events, such as upper respiratory tract infections or herpes zoster (25,52). As such, careful safety monitoring of patients treated with povetacicept will be warranted during its clinical trials, hopefully affording eventual determination of a potently effective yet safe dosing regimen.

The potent immunosuppressive activity of povetacicept in vitro and in spontaneous and inducible models of SLE (Figures 2 and 5) suggests it could be a superior therapeutic candidate in B cell–related autoimmune diseases, in which both APRIL and BAFF are dysregulated, and in settings where pathogenic autoantibodies contribute to disease progression. Whereas rituximab is used in standard practice in off-label settings, TACI is expressed on a broader range of B cell and plasma cell subsets compared to CD20, particularly antibody-producing plasmablasts and plasma cells. Since these ASCs are considered the primary source of pathogenic autoantibodies in SLE, combined inhibition of BAFF and APRIL with povetacicept has potential for greater efficacy. In addition to SLE, antibody-associated glomerular diseases including LN and IgA nephropathy, as well as autoantibody-associated dermatoses, hematologic diseases, and neurologic diseases, might be better controlled with povetacicept treatment.

The limitations of these studies relate to the inherent caveats associated with animal models of human disease. Mouse lupus models cannot fully reproduce human clinical pathology; however, the NZB/NZW mouse lupus model is well regarded as a tool for evaluating therapeutic candidates, since it develops spontaneously and with several, though not all, characteristics similar to those observed in lupus patients (18,19,53). In our study, dosing began when the NZB/NZW mice were 22 weeks old, when mice typically start displaying signs of lupus. However, markers of disease activity such as anti-dsDNA antibodies and proteinuria were still relatively low at that stage, and therefore, the dosing regimen we evaluated cannot be considered fully therapeutic and instead better represents an "early intervention" regimen. In the mouse KLH and SRBC immunization models, povetacicept dosing resulted in a significantly lower number of plasma cells, though because dosing occurred early in the models, the observed plasma cell reduction may be due to a blockade in plasma cell generation rather than effects on the survival of existing plasma cells, as this was not directly evaluated in our experiments. Future studies are planned to evaluate the impact of povetacicept on recall responses and on memory B cells that upon reactivation can develop into antibody-producing, short-lived plasma cells.

Additionally, we have defined long-lived plasma cells in our mouse studies using a previously described immunophenotype (i.e., viable TACI$^{high}$CD138$^{high}$B220–CD19– cells) (54), though we did not formally confirm the functionality of cells bearing this phenotype in our experiments. Future studies could include, for example, adoptive transfer experiments with tagged or labeled B cells as a more definitive way to define and track long-lived plasma cells following immunization. Finally, it should also be noted that the evaluation of povetacicept in the primary human B cell assay may not fully reflect the effects of treatment in humans. Nevertheless, the correlation between the observed activity of povetacicept in the mouse models and in the human primary B cell assay support the potential clinical translatability of our results.

Povetacicept was designed to overcome the shortcomings of BAFF- or APRIL-specific inhibitors and improve the affinity of WT TACI toward APRIL. By targeting both BAFF and APRIL, povetacicept has the potential to achieve superior efficacy in heterogeneous autoimmune disease settings such as SLE. Clinical trials of povetacicept in B cell–related and autoantibody-related autoimmune diseases are strongly warranted and will enable the first clinical evaluation of potent coinhibition of both APRIL and BAFF. A phase I trial of povetacicept in healthy adult volunteers (ClinicalTrials.gov identifier: NCT05034484) has been initiated to enable such studies (55).

## ACKNOWLEDGMENTS

The authors thank our colleagues, past and present, at Alpine Immune Sciences and particularly Steve Levin, Sean MacNeil, Wayne Gombotz, Josiah Brown, Mike Salema, Leah Zielinski, Andrea Peng, Chelsea Gudgeon, Erika Rickel, Kristine Swiderek, Mark Maurer, Jason Stubrich, and Jan Hillson for their contributions to the development of povetacicept. We gratefully acknowledge Olympic Protein Sciences for performing the surface plasmon resonance analyses, Hooke Laboratories for conducting the NZB/NZW study, Altasciences for conducting the cynomolgus monkey pharmacokinetics/pharmacodynamics study, and Kelly Byrnes-Blake for analyzing the pharmacokinetic data. We also gratefully acknowledge the medical writing/editing support of Julie Crider, Nan Luo, and Kristen Howery.

## AUTHOR CONTRIBUTIONS

All authors were involved in drafting the article or revising it critically for important intellectual content. All authors approved the final version to be published. Mr. Evans and Dr. Lewis had full access to all the data in the study and take responsibility for the integrity of the data and the accuracy of the data analysis.

**Study conception and design.** Evans, Lewis, DeMonte, Wolfson, Dillon, Mudri, Yang, Peng, Rixon.

**Acquisition of data.** Evans, Lewis, Wolfson, Mudri, Kleist, Griffin, Hong, Hebb, Messenheimer, Wang, Seaberg, Bhandari, Garrett, Kuijper, Ardourel, Debrot.

**Analysis and interpretation of data.** Evans, Lewis, DeMonte, Dillon, Holland, Rixon, Peng, Yang, Sanderson, Chunyk Mudri, Kleist, Wang, Seaberg, Debrot.

## ADDITIONAL DISCLOSURE

All authors of this article are current or former employees of Alpine Immune Sciences, Inc.

## REFERENCES


1. Lund FE. Cytokine-producing B lymphocytes—key regulators of immunity [review]. Curr Opin Immunol 2008;20:332–8.
2. Banchereau R, Hong S, Cantarel B, et al. Personalized immunomonitoring uncovers molecular networks that stratify lupus patients [published correction appears in Cell 2016;165:1548–50]. Cell 2016;165: 551–65.
3. Samy E, Wax S, Huard B, et al. Targeting BAFF and APRIL in systemic lupus erythematosus and other antibody-associated diseases [review]. Int Rev Immunol 2017;36:3–19.
4. Eslami M, Schneider P. Function, occurrence and inhibition of different forms of BAFF [review]. Curr Opin Immunol 2021;71:75–80.
5. Roschke V, Sosnovtseva S, Ward CD, et al. BLyS and APRIL form biologically active heterotrimers that are expressed in patients with systemic immune-based rheumatic diseases. J Immunol 2002;169: 4314–21.
6. Dillon SR, Harder B, Lewis KB, et al. B-lymphocyte stimulator/a proliferation-inducing ligand heterotrimers are elevated in the sera of patients with autoimmune disease and are neutralized by atacicept and B-cell maturation antigen-immunoglobulin. Arthritis Res Ther 2010;12:R48.
7. Hahn BH. Belimumab for systemic lupus erythematosus [review]. N Engl J Med 2013;368:1528–35.
8. Asif S, Bargman J, Auguste B. A review of the AURORA and BLISS trials: will it revolutionize the treatment of lupus nephritis? [review]. Curr Opin Nephrol Hypertens 2022;31:278–82.
9. Oon S, Huq M, Golder V, et al. Lupus Low Disease Activity State (LLDAS) discriminates responders in the BLISS-52 and BLISS-76 phase III trials of belimumab in systemic lupus erythematosus. Ann Rheum Dis 2019;78:629–33.
10. Furie R, Rovin BH, Houssiau F, et al. Two-year, randomized, controlled trial of belimumab in lupus nephritis. N Engl J Med 2020;383: 1117–28.
11. McWilliams EM, Lucas CR, Chen T, et al. Anti-BAFF-R antibody VAY-736 demonstrates promising preclinical activity in CLL and enhances effectiveness of ibrutinib. Blood Adv 2019;3:447–60.
12. Dulos J. BION-1301: a novel fully blocking APRIL antibody for the treatment of multiple myeloma. Presented at the annual meeting of the America Society of Hematology; 2016; San Diego, California.
13. Myette JR, Kano T, Suzuki H, et al. A proliferation inducing ligand (APRIL) targeted antibody is a safe and effective treatment of murine IgA nephropathy. Kidney Int 2019;96:104–16.
14. Barratt J. Pharmacodynamic and clinical responses to BION-1301 in patients with IgA nephropathy: initial results of a Ph1/2 trial [abstract]. Presented at meeting of the American Society of Nephrology; November 4, 2021; virtual meeting. URL: https://www.asn-online.org/education/kidneyweek/2021/program-abstract.aspx?controlId=3602629.
15. Mathur M, Barratt J, Suzuki Y, et al. Safety, tolerability, pharmacokinetics, and pharmacodynamics of VIS649 (sibeprenlimab), an APRIL-neutralizing $IgG_2$ monoclonal antibody, in healthy volunteers. Kidney Int Rep 2022;7:993–1003.
16. Ramanujam M, Wang X, Huang W, et al. Similarities and differences between selective and nonselective BAFF blockade in murine SLE. J Clin Invest 2006;116:724–34.
17. Benson MJ, Dillon SR, Castigli E, et al. Cutting edge: the dependence of plasma cells and independence of memory B cells on BAFF and APRIL. J Immunol 2008;180:3655–9.
18. Haselmayer P, Vigolo M, Nys J, et al. A mouse model of systemic lupus erythematosus responds better to soluble TACI than to soluble BAFFR, correlating with depletion of plasma cells. Eur J Immunol 2017;47:1075–85.
19. Huard B, Tran NL, Benkhoucha M, et al. Selective APRIL blockade delays systemic lupus erythematosus in mouse. PLoS One 2012;7: e31837.
20. Liu Z, Davidson A. BAFF inhibition: a new class of drugs for the treatment of autoimmunity [review]. Exp Cell Res 2011;317:1270–7.
21. Stohl W, Yu N, Chalmers S, et al. Development of murine systemic lupus erythematosus in the absence of BAFF. Arthritis Rheumatol 2020;72:292–302.
22. Zhou B, Zhang H, Su X, et al. Therapeutic effects of a novel BAFF blocker on arthritis. Signal Transduct Target Ther 2019;4:19.
23. Shi F, Xue R, Zhou X, et al. Telitacicept as a BLyS/APRIL dual inhibitor for autoimmune disease [review]. Immunopharmacol Immunotoxicol 2021;43:666–73.
24. Merrill JT, Wallace DJ, Wax S, et al. Efficacy and safety of atacicept in patients with systemic lupus erythematosus: results of a twenty-four-week, multicenter, randomized, double-blind, placebo-controlled, parallel-arm, phase IIb study [published corrections appear in Arthritis Rheumatol 2018;70:467 and Arthritis Rheumatol 2021;73:2043]. Arthritis Rheumatol 2018;70:266–76.
25. Dhillon S. Telitacicept: first approval [review]. Drugs 2021;81:1671–5.
26. Vera Therapeutics. Vera therapeutics provides business update and reports second quarter 2022 financial results. August 10, 2022. Accessed March 17, 2023. URL: https://www.globenewswire.com/news-release/2022/08/10/2495661/0/en/Vera-Therapeutics-Provides-Business-Update-and-Reports-Second-Quarter-2022-Financial-Results.html.
27. Wu D, Li J, Xu D, et al. Telitacicept, a human recombinant fusion protein targeting B lymphocyte stimulator (BlyS) and a proliferation-inducing ligand (APRIL), in systemic lupus erythematosus (SLE): Results of a Phase 3 Study [abstract]. Presented at American College of Rheumatology Convergence 2022; October 18, 2022. URL: https://acrabstracts.org/abstract/telitacicept-a-human-recombinant-fusion-protein-targeting-b-lymphocyte-stimulator-blys-and-a-proliferation-inducing-ligand-april-in-systemic-lupus-erythematosus-sle-results-of-a-phase-3-study/.
28. Schuepbach-Mallepell S, Das D, Willen L, et al. Stoichiometry of heteromeric BAFF and APRIL cytokines dictates their receptor binding and signaling properties. J Biol Chem 2015;290:16330–42.
29. Levin SD, Evans LS, Bort S, et al. Novel immunomodulatory proteins generated via directed evolution of variant IgSF domains. Front Immunol 2020;10:3086.
30. Kelkka T, Kienhöfer D, Hoffmann M, et al. Reactive oxygen species deficiency induces autoimmunity with type 1 interferon signature. Antioxid Redox Signal 2014;21:2231–45.
31. Klarquist J, Janssen EM. The bm12 inducible model of systemic lupus erythematosus (SLE) in C57BL/6 mice. J Vis Exp 2015:e53319.
32. Hymowitz SG, Patel DR, Wallweber HJA, et al. Structures of APRIL-receptor complexes: like BCMA, TACI employs only a single cysteine-rich domain for high affinity ligand binding. J Biol Chem 2005;280:7218–27.
33. Hezareh M, Hessell AJ, Jensen RC, et al. Effector function activities of a panel of mutants of a broadly neutralizing antibody against human immunodeficiency virus type 1. J Virol 2001;75:12161–8.
34. Dixon FJ, Andrews BS, Eisenberg RA, et al. Etiology and pathogenesis of a spontaneous lupus-like syndrome in mice. Arthritis Rheum 1978;21:S64–7.

35. Carbonatto M, Yu P, Bertolino M, et al. Nonclinical safety, pharmacokinetics, and pharmacodynamics of atacicept. Toxicol Sci 2008;105: 200–10.
36. Merrill JT, Neuwelt CM, Wallace DJ, et al. Efficacy and safety of rituximab in moderately-to-severely active systemic lupus erythematosus: the randomized, double-blind, phase II/III systemic lupus erythematosus evaluation of rituximab trial. Arthritis Rheum 2010; 62:222–33.
37. Rovin BH, Furie R, Latinis K, et al. Efficacy and safety of rituximab in patients with active proliferative lupus nephritis: the Lupus Nephritis Assessment with Rituximab study. Arthritis Rheum 2012;64: 1215–26.
38. Lee DSW, Rojas OL, Gommerman JL. B cell depletion therapies in autoimmune disease: advances and mechanistic insights [review]. Nat Rev Drug Discov 2021;20:179–99.
39. Gross JA, Dillon SR, Mudri S, et al. TACI-Ig neutralizes molecules critical for B cell development and autoimmune disease. impaired B cell maturation in mice lacking BLyS. Immunity 2001;15: 289–302.
40. Castigli E, Scott S, Dedeoglu F, et al. Impaired IgA class switching in APRIL-deficient mice. Proc Natl Acad Sci USA 2004;101:3903–8.
41. Zhai YL, Zhu L, Shi SF, et al. Increased APRIL expression induces IgA1 aberrant glycosylation in IgA nephropathy. Medicine (Baltimore) 2016;95:e3099.
42. Barratt J, Kooienga L, Hour B, et al. Updated interim results of a phase 1/2 study to investigate the safety, tolerability, pharmacokinetics, pharmacodynamics, and clinical activity of BION-1301 in patients with IgA nephropathy [abstract]. Nephrol Dial Trans 2022;37: gfac067.011.
43. Morand EF, Furie R, Tanaka Y, et al. Trial of anifrolumab in active systemic lupus erythematosus. N Engl J Med 2020;382:211–21.
44. Deeks ED. Anifrolumab: first approval [review]. Drugs 2021;81: 1795–802.
45. Morales S, Cross J, Huizinga R. An improved BAFF/APRIL inhibitor with increased potency and safety for the treatment of B cell–mediated diseases [abstract]. Presented at American College of Rheumatology Convergence 2022; November 14, 2022. URL: https://acrabstracts.org/abstract/aur200-an-improved-baff-april-inhibitor-with-increased-potency-and-safety-for-the-treatment-of-b-cell-mediated-diseases/.
46. Miao YR, Thakkar K, Cenik C, et al. Developing high-affinity decoy receptors to treat multiple myeloma and diffuse large B cell lymphoma. J Exp Med 2022;219:e20220214.
47. Tudesq JJ, Cartron G, Rivière S, et al. Clinical and microbiological characteristics of the infections in patients treated with rituximab for autoimmune and/or malignant hematological disorders [review]. Autoimmun Rev 2018;17:115–24.
48. Marco H, Smith RM, Jones RB, et al. The effect of rituximab therapy on immunoglobulin levels in patients with multisystem autoimmune disease. BMC Musculoskelet Disord 2014;15:178.
49. Varley CD, Winthrop KL. Long-term safety of rituximab (risks of viral and opportunistic infections) [review]. Curr Rheumatol Rep 2021; 23:74.
50. Kaegi C, Steiner UC, Wuest B, et al. Systematic review of safety and efficacy of atacicept in treating immune-mediated disorders. Front Immunol 2020;11:433.
51. Ginzler EM, Wax S, Rajeswaran A, et al. Atacicept in combination with MMF and corticosteroids in lupus nephritis: results of a prematurely terminated trial. Arthritis Res Ther 2012;14:R33.
52. Telitacicept for injection [package insert]. Shandong, China: Rongchang Biopharmaceutical (Yantai) Co., Ltd.; 2021.
53. Cornaby C, Elshikha AS, Teng X, et al. Efficacy of the combination of metformin and CTLA4Ig in the (NZB × NZW)F1 mouse model of lupus nephritis. Immunohorizons 2020;4:319–31.
54. Pracht K, Meinzinger J, Daum P, et al. A new staining protocol for detection of murine antibody-secreting plasma cell subsets by flow cytometry. Eur J Immunol 2017;47:1389–92.
55. Dillon S, Harrison P, Lickliter J, et al. A randomized placebo-controlled phase 1 study in healthy adult volunteers of the safety, tolerability, pharmacokinetics, and pharmacodynamics of ALPN-303, a potent dual BAFF/APRIL antagonist for the treatment of systemic lupus erythematosus and other autoantibody-associated diseases [abstract]. Presented at American College of Rheumatology Convergence 2022; November 13, 2022. URL: https://acrabstracts.org/abstract/a-randomized-placebo-controlled-phase-1-study-in-healthy-adult-volunteers-of-the-safety-tolerability-pharmacokinetics-and-pharmacodynamics-of-alpn-303-a-potent-dual-baff-april-antagonist-for-the-t/.